(Received 29 November 2024, Accepted 13 February 2025, Scheduled 3 March 2025)

Study on the Application of Improved Fuzzy Adaptive Control on PMSM System

Xuhong Yang[1], Chenhao Li[1,*], Sujie Zhang[2], and Fengwei Qian[3]

[1] College of Automation Engineering, Shanghai University of Electric Power, Shanghai 200090, China
[2] State Grid Shanghai Municipal Electric Power Company, Shanghai 200122, China
[3] Shanghai Solar Energy Research Center, Shanghai 200240, China

ABSTRACT: Aiming at the problem of low robustness of fuzzy adaptive control when it is applied to permanent magnet synchronous motor system (PMSM), the study introduced the sliding film control method to optimize it, so as to enhance the robustness of PMSM. The results demonstrated that the torque error of the adaptive fuzzy sliding mode control (AFSMC) was 1.86 Nm, which is 62.8% and 38% less than the peak torque pulsation of 5 Nm and 3 Nm for the fuzzy adaptive control, respectively, and indicates a better steady-state capability when the motor is operated at 1500 rpm and 30 Nm load. In addition, in the robustness validation experiments, under the initial stage, the two methods have the same rotational speed response, but after the parameter changes, the AFSMC adjusts quickly, while the traditional fuzzy adaptive control responds slowly. Moreover, under the same load inertia, the AFSMC exhibits smaller overshoot and faster regulation, smaller speed fluctuation and faster recovery during load surge. In complex scenarios, AFSMC reduces recovery time by 60% over traditional control methods, which demonstrates that the fuzzy adaptive sliding film control proposed by the study is successful in enhancing the system's stability and capability when the PMSM is applied.

1. INTRODUCTION

As the processing capability of automated control devices such as industrial robots increases, so do the requirements for accuracy and stability of motor control [1]. PMSM is widely adopted in the field of high performance machine tools and industrial control robots because of its high power factor, high energy efficacy, and adjustable parameters [2]. Given that the PMSM is a complex time-varying system, the traditional proportion integration differentiation (PID) controller is challenging to fulfill the demand for strong robustness and fast response, so in recent times there has been a growing number of researches on the control methods of PMSM, to further improve the control effect [3]. These advanced control algorithms include sliding mode (SM) variable structure control, fuzzy adaptive (FA) control, and intelligent control. Among them, FA control is more convenient in obtaining the dynamic characteristics of the controlled object and easy to learn in immediate time because of the introduction of the adaptive rate. Besides, FA control has lower requirements for the mathematical model of the control object. Grounded on the above characteristics, FA control has good effect in the application of permanent magnet motor [4, 5]. At the same time, FA has a problem of low robustness. So the study introduces SM control to optimize FA to achieve its overall robustness when it is applied to PMSM.

The innovation of the study is to integrate SM control technique into FA control strategy, which enhances the stability of the PMSM in the face of parameter variations and external load fluctuations, and improves the system robustness. The proposed method of the study has obvious advantages in steady state and dynamic performance, especially in reducing torque error, lowering speed fluctuation, and speeding up the system response. These results not only demonstrate the innovation of the proposed method in control strategy, but also provide a new solution for high performance control of PMSM.

The study is organized into four sections. The second section is to summarize and discuss the research on FA control and PMSM. The third section is to construct a PMSM model and optimize the FA algorithm using sliding film control. The fourth section is to verify the application effect of FA sliding film control in PMSM. The fifth section is to summarize the whole article.

2. RELATED WORKS

Xu et al. developed a novel stabilizing control strategy to address a type of interconnected systems that exhibit nonlinearity, which are vulnerable to unaccounted-for dynamics and unpredictable states. The scheme was designed to address the issue that these systems are susceptible to unmodeled dynamics and surprising states. The plan built a state observer to correct the system interconnections using a cyclic small gain condition theorem and used a system utilizing fuzzy logic to estimate the unidentified function [6]. Sui and other scholars studied the finite time FA event-triggered control design problem with unmodeled dynamics. The study established new event-triggered FA finite time based control algorithms, used a fuzzy logic system to find unknown nonlinearities, and created state observers to estimate the unmeasured states. It also demonstrated prob-

* Corresponding author: Chenhao Li (shiep_lch067@163.com).

abilistic semiglobal finite time stability of the closed-loop system by utilizing a dynamic signal function to handle the unmodeled dynamics [7]. Huang and his team members proposed a generalized fuzzy neural network based control strategy for dealing with robot environment interaction under unknown environmental influences. The strategy solved the neural network selection problem through a generalized learning system to have adaptive impedance training to achieve the best possible interaction between the robot and its surroundings [8]. To improve the H∞ adaptive tracking performance, Yang et al. created multiple segmented stochastic Liapunov functions and designed combined switching rule and fuzzy dynamic adaptive switching strategy for the H∞ stochastic tracking control issue of uncertain fuzzy Markov hybrid switching system [9]. Utilizing a fuzzy logic system, Zong and his colleagues examined the autonomous underwater vehicle's longitudinal dynamics and its robust adaptive control. The target tracking command was converted to the pitch angle command using dynamic transformation, and a tracking controller that combined a robust design and fuzzy logic system was created. Liapunov analysis was used to demonstrate the consistent limit-bounded stability [10].

In addition to this, for a class of nonlinear systems with saturated inputs, Ren et al. used a dynamic event triggering mechanism for alleviating the system's workload and applied the mechanism in the design of the controller by using inversion techniques. After Ljapunov stability analysis, the study demonstrated that all signals in the feedback control system remained within a certain limit [11]. Aiming at the control problem of PMSM speed servo system under various disruptions, Zheng and other scholars proposed a fractional-order SM control method. The PMSM speed servo's centralized exogenous disturbances and uncertainties were assessed using an extended state observer and an enhanced disturbance observer. The validity and benefits of the suggested approach are proved following PMSM speed control tests and comparison with a few current approaches [12]. Rafaq and his team members studied torque pulsation minimization techniques for PMSM, analyzed the sources of torque pulsations, and discussed the drawbacks of torque measurement techniques [13]. Regarding the problem of optimizing the controller parameters of PMSM, Fang et al. proposed an improved hybrid particle swarm optimization (PSO) algorithm. The algorithm raises the searching ability by directional variational operation and improved particle velocity updating formula, and is applied to optimize the velocity and position controller parameters to confirm the validity of the hybrid PSO algorithm and the designed control system [14]. Yu and other scholars compared the performance of PMSM and permanent magnet vernier machine systems in in-wheel direct drive applications, analyzed the performance of the two motors from the theoretical and experimental perspectives, and discussed their advantages and disadvantages for the advancement of high-efficiency wheel-driven systems for electric vehicles [15].

From the above research, it is indicated that the current for the application of FA in permanent magnet motor has the problem of low robustness, so the study of the use of sliding film control is carried out to optimize the FA to improve its robustness.

3. MATHEMATICAL MODEL CONSTRUCTION AND FA IMPROVEMENT OF PMSM

3.1. PMSM Model Construction

In an electrically excited three-phase synchronous motor, the rotor consists of an excitation coil, whereas in a PMSM, the rotor is replaced by a permanent magnet, which is the reason for its name [16]. Permanent magnets are categorized in different ways depending on how they are configured on the rotor. They can be categorized into three main types, namely, built-in, inserted, and surface-mounted ones. Among them, surface-mounted PMSMs are also known as hidden pole synchronous motors because their permeability is close to that of air, so there is not much difference between straight-axis and cross-axis inductance [17]. The straight-axis inductance of the other two types of PMSM is smaller than the cross-axis inductance, and the reluctance torque will also be generated along with the electromagnetic torque, which is different from the surface-mounted PMSM. To control the PMSM more accurately, the study establishes a mathematical model based on its strong coupling and nonlinear characteristics. Taking the three-phase two-pole PMSM as an example, its structure is as shown in Fig. 1.

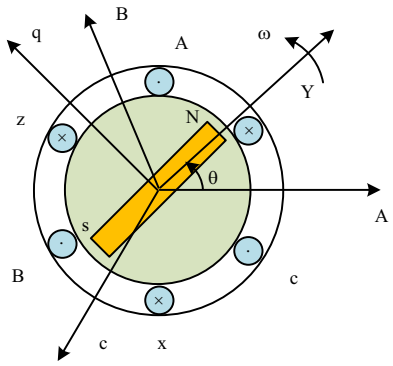

FIGURE 1. Structure of three-phase two-pole PMSM.

Although the rotor structure of a PMSM is broadly similar to that of a three-phase two-pole synchronous motor (SYM), there are differences. While the rotor magnetic field strength of a three-phase SYM is adjusted as the current changes, the rotor magnetic field strength of a PMSM is fixed at the time of manufacture, meaning that its rotor magnetic chain remains constant [18]. When the rotor magnetic chain is always rotating in synchronization with the stator magnetic chain and maintains a phase difference of 90 degrees electrical angle, a maximum electromagnetic torque is generated, thus ensuring that the stator magnetic potential is applied to the rotor with maximum efficiency. To achieve precise control of the motor, it is investigated to convert the three-phase currents to the α-β coordinate system (CS). An orthogonal two-phase CS where the α-axis and the A-phase coincide is called α-β CS, and the β-axis is perpendicular to the α-axis and is located between the A-phase and B-phase. With this transformation, quantities in a three-phase stationary CS (SCS) can be converted to quantities in a two-phase SCS while ensuring that the magnetic potential remains equivalent. This transformation is usually realized by

the Clarke transform, whose transformation formula is in Eq. (1).

$$\begin{bmatrix} i_\alpha \\ i_\beta \end{bmatrix} = \frac{2}{3}\begin{bmatrix} 1 & -1\backslash 2 & -1\backslash 2 \\ 0 & \sqrt{3}\backslash 2 & -\sqrt{3}\backslash 2 \end{bmatrix}\begin{bmatrix} i_a \\ i_b \\ i_c \end{bmatrix} \quad (1)$$

In Eq. (1), i_α and i_β denote the stator currents on the α and β axes. i_a, i_b, and i_c denote the stator currents on the a, b, and c axes, respectively. To determine the α- and β-axis components of the ABC three-phase SCS, a current orthogonal decomposition is performed in the α-β two-phase SCS. The Clark inverse transformation is in Eq. (2).

$$\begin{bmatrix} i_a \\ i_b \\ i_c \end{bmatrix} = \begin{bmatrix} 1 & 0 \\ -1\backslash 2 & \sqrt{3}\backslash 2 \\ -1\backslash 2 & -\sqrt{3}\backslash 2 \end{bmatrix}\begin{bmatrix} i_\alpha \\ i_\beta \end{bmatrix} \quad (2)$$

In the α-β CS, the stator voltage equation is as Eq. (3).

$$\begin{bmatrix} u_\alpha \\ u_\beta \end{bmatrix} = \begin{bmatrix} R+\frac{d}{dt}L_\alpha & \frac{d}{dt}L_{\alpha\beta} \\ \frac{d}{dt}L_{\alpha\beta} & R+\frac{d}{dt}L_\beta \end{bmatrix}\begin{bmatrix} i_\alpha \\ i_\beta \end{bmatrix} + \omega\Psi_f \begin{bmatrix} -\sin\theta \\ \cos\theta \end{bmatrix} \quad (3)$$

In Eq. (3), u_α and u_β denote the stator voltage on the α and β axes, respectively; L_α and L_β denote the self-inductance on the α and β axes, respectively; $L_{\alpha\beta}$ denotes the mutual inductance between the α and β axes; R denotes the resistance of the stator windings; $\frac{d}{dt}$ denotes the derivative with respect to time, i.e., the rate of change; ω denotes the motor angular velocity; Ψ_f denotes the rotor magnetic chain; and θ denotes the rotor position angle. The specific variables are calculated as in Eq. (4).

$$\begin{cases} L_\alpha = L_0 + L_1\cos 2\theta \\ L_\beta = L_0 + L_1\cos 2\theta \\ L_{\alpha\beta} = L_1\sin 2\theta \\ L_0 = (L_d + L_q)/2 \\ L_1 = (L_d - L_q)/2 \end{cases} \quad (4)$$

In Eq. (4), L_0 and L_1 denote the two parameters of the motor self-inductance. L_d and L_q denote the motor's cross-axis and direct-axis inductances, respectively. To simplify the analysis of the physical characteristics of the motor, Park transformation is used in the study. Park transformation is as in Eq. (5).

$$\begin{bmatrix} i_d \\ i_q \end{bmatrix} = \begin{bmatrix} \cos\theta_r & \sin\theta_r \\ -\sin\theta_r & \cos\theta_r \end{bmatrix}\begin{bmatrix} i_\alpha \\ i_\beta \end{bmatrix} \quad (5)$$

In Eq. (5), the simplified control of the PM SYM is mainly achieved by obtaining the current sum versus rotor position. That is, the current components on the α-β axis are decomposed by combining the angle of the A-phase with the rotor and mapped in the d-q axis. The d-axis is in line with the rotor's flux direction in the d-q CS, which is a rotating CS, while the q-axis is perpendicular to the d-axis and rotates synchronously with the rotational direction of the rotor. The torque of a PMSM can be regulated by adjusting the current strength in the d-q axis. In the d-axis, current i_d mainly affects the magnetic flux of the motor, while in the q-axis, current i_q mainly affects the torque of the motor. By adjusting the magnitude of i_q, achieving accurate regulation of motor torque is possible, thus making the PMSM exhibit performance characteristics similar to those of a DC motor, so that it is capable of fast and precise torque and speed control. At this point, the control of the torque of the PM SYM can be achieved by adjusting the current strength in the d-q axis and make it exhibit the performance characteristics similar to that of a DC motor. Park inverse transformation is as Eq. (6).

$$\begin{bmatrix} i_\alpha \\ i_\beta \end{bmatrix} = \begin{bmatrix} \cos\theta_r & -\sin\theta_r \\ -\sin\theta_r & \cos\theta_r \end{bmatrix}\begin{bmatrix} i_d \\ i_q \end{bmatrix} \quad (6)$$

After completing the coordinate transformation, in the PMSM model, the stator voltage equation is as Eq. (7).

$$\begin{cases} u_d = Ri_d + p\psi_d - \omega\psi_q \\ u_q = Ri_q + p\psi_q - \omega\psi_d \end{cases} \quad (7)$$

In Eq. (7), p denotes the differential operator. The stator magnetic chain equation is as in Eq. (8).

$$\begin{cases} \psi_d = \psi_f + L_d i_d \\ \psi_q = L_q i_q \end{cases} \quad (8)$$

The electromagnetic torque equation is as in Eq. (9).

$$T_e = \frac{3}{2}n_p\left[\psi_f i_q + (L_d - L_q)i_d i_q\right] \quad (9)$$

For surface-mounted PMSM, the calculation of the electromagnetic torque can be streamlined as in Eq. (10) due to the equal cross-axis and straight-axis inductances.

$$T_e = \frac{3}{2}n_p\psi_f i_q \quad (10)$$

The equation of motion is as Eq. (11).

$$T_e - T_1 = \frac{J}{n_p}\frac{d\omega}{dt} \quad (11)$$

In the CS of d-q, the electromagnetic torque of a PMSM is only determined by the cross-axis current i_q, which is independent of the straight-axis current i_d. For surface-mounted motors, the torque magnitude is proportional to i_q. This simplifies the control process and possesses the benefits of high power density, low rotational inertia, and brushless structure. Although PMSMs are highly responsive and accurately controlled, their performance is susceptible to system perturbations. Therefore, the reduction of these disturbances is essential to achieve accurate motor control.

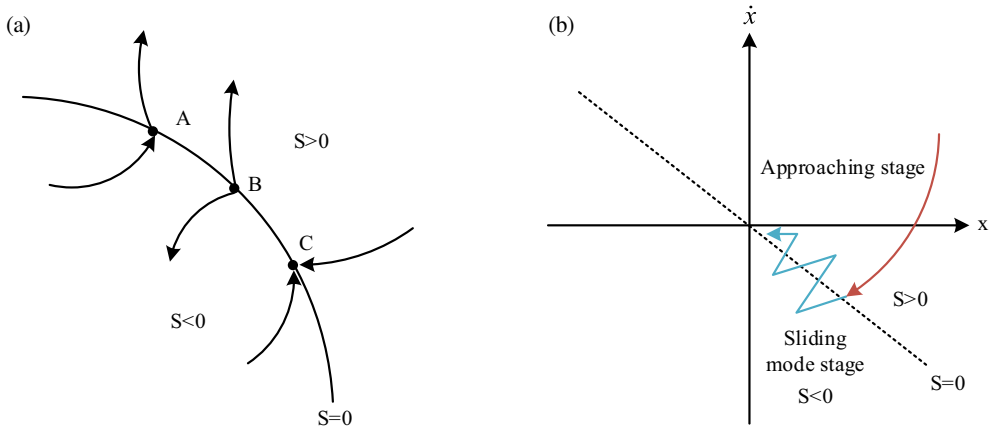

FIGURE 2. Schematic diagram of SM control principle. (a) Schematic diagram of distribution of sliding surface. (b) Schematic diagram of sliding mode motion process.

3.2. FA Improvement Combined with SM Control

Fuzzy logic control is able to mimic the human decision-making process and is a rule-based control method; therefore, a precise mathematical model is not necessary. Through the three steps of fuzzification, rule-based reasoning and defuzzification, fuzzy controllers are able to handle uncertainty and nonlinear problems [19]. However, it may lack sufficient precision and adaptability in dealing with complex systems. Adaptive control, on the other hand, is a control strategy that can automatically adjust the control parameters according to the system performance. It is able to cope with the uncertainties and variations of system parameters and keep the system performance in the optimal state through online estimation and adjustment [20]. FA control, which integrates the two, is a fuzzy logic-based control technique that processes and regulates nonlinear systems using fuzzy logic reasoning, fuzzy linguistic variables, and fuzzy set theory [21, 22]. By automatically modifying the controller parameters, FA control is used in PMSM control systems to increase the system's dynamic stability and adapt to various operating situations. However, the disadvantage of this approach is that while it simplifies the control process, it lacks robustness. Therefore, it is investigated to introduce SM control to enhance the system robustness. SM control is one of the extremely effective control strategies for dealing with high levels of system uncertainty, which essentially involves directing the state of the system towards one or more specific surfaces, known as SM surfaces, which are designed to move in a predetermined manner until it approaches zero through the use of intermittent control signals and ensuring that the state moves in a predetermined manner on these surfaces [23]. The principle of SM control is shown in Fig. 2.

The conventional SM control design involves selecting the SM surface to determine the desired system performance and applying discontinuous control signals to ensure that these performance objectives are met, as in Fig. 3.

The number of input variables decides the dimensionality of the fuzzy system, such as a one, two, or three dimensional fuzzy control system, whereas the accuracy and complexity of the fuzzy controller increase with the dimensionality, and the

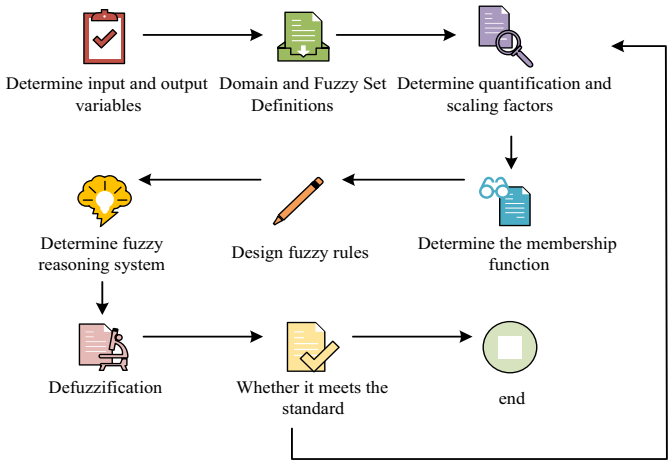

FIGURE 3. Design process of fuzzy SM controller.

computation time also increases. Considering these factors, the study selects a two-dimensional fuzzy controller, i.e., with two input variables: fuzzy coefficients m_1 and m_2. Such a design aims at balancing the control accuracy and arithmetic difficulty, so as to ensure an adequate control effect. The fuzzy control rate is as Eq. (12).

$$u_b^* = -\frac{1}{k_m}\left(m_1 k_1 s + m_2 k_2 |s|^{\gamma 2}\right) \text{sign}(s)) \tag{12}$$

To improve the control accuracy, clear physical quantities s, m_1, and m_2 need to be fuzzified into fuzzy sets. The careful division of the fuzzy domain can improve the accuracy, but at the same time, it will increase the computational complexity and memory requirements. Therefore, the study chooses to divide the fuzzy theoretical domain into 5 grades, and the specific fuzzy set is as Eq. (13).

$$\begin{cases} s = \{Z, PS, PM, PNB, PB\} \\ m_1 = \{Z, PS, PM, PNB, PB\} \\ m_2 = \{Z, PS, PM, PNB, PB\} \end{cases} \tag{13}$$

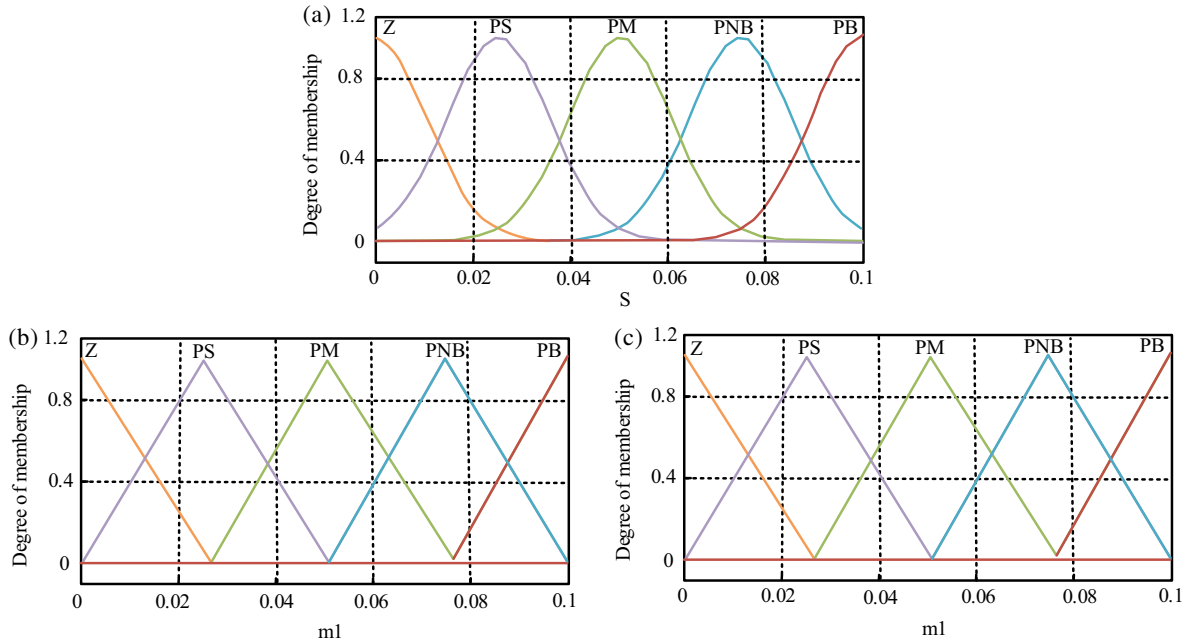

FIGURE 4. Membership function curves of each variable. (a) The membership function of s. (b) The membership function of m_1. (c) The membership function of m_2.

In Eq. (13), the physical domain of s is [0, 0.1], and the physical domain of m_1 and m_2 is [0, 1]. Z denotes the zero in the fuzzy linguistic variable. PS denotes positively small, PM positively medium, PNB nearly positively large, and PB positively large. In fuzzy controllers, the physical domain of the output variable changes due to changes in the reference signal and controller parameters, but the fuzzy domain is fixed and affects the control effect, so it is investigated to adjust the proportionality of the input and output signals to the fuzzy domain using quantization and proportionality factors to ensure the performance of the controller. The factor values are in Table 1.

TABLE 1. Quantitative factor and scale factor values.

Reference signal	Quantitative factors q_s	Quantitative factors q_1	Quantitative factors q_2
Step signal	1	4	1.4
Sinusoidal signal	2	4	1.4

To perform the fuzzification operation, an affiliation function is required. The affiliation function is a mathematical tool used to characterize a fuzzy set. It describes the affiliation of a fuzzy set, e.g., element u to U. Due to the indistinguishable nature of this relationship, the affiliation function uses values in an interval to describe the "true degree" to which an element belongs to a fuzzy set. Since the computation process may change depending on the function, the input variables should be optimized to reduce the computational effort, displayed in Fig. 4.

As can be seen from Fig. 4(a), the study sets the affiliation function of s as Gaussian type, while Figs. 4(b) and (c) show the affiliation functions of m_1 and m_2, which are both triangular type. The Gaussian-type affiliation function is an affiliation function based on a Gaussian distribution, which is usually used in fuzzy logic systems to describe the affiliation relationship between input values and fuzzy sets. It has a smooth curve shape and is suitable for fuzzy systems that require smooth transitions. Triangular affiliation function is a simple affiliation function with a triangular shape, which is characterised by its simple shape and high computational efficiency. When setting the fuzzy rules, it is usually necessary to optimize them through repeated trials and adjustments to ensure that the control system shows good performance under various operating conditions. In the study, the fuzzy rules are set as shown in Table 2, taking into account the system response speed and vibration jitter while combining expert knowledge.

TABLE 2. Fuzzy rule table.

$\|s\|$	m_1	m_2
Z	PB	Z
PS	PNB	PS
PM	PM	PM
PNB	PS	PNB
PB	Z	PB

In view of the study's high demand for control accuracy, the study chooses to obtain the fuzzy output results through the center of gravity method. The method of center of gravity is a commonly used defuzzification technique, and its advantage lies in its ability to better deal with the shape and distribution of the fuzzy output set and to obtain a reasonably accurate output value even in the case of overlapping or dispersed output sets.

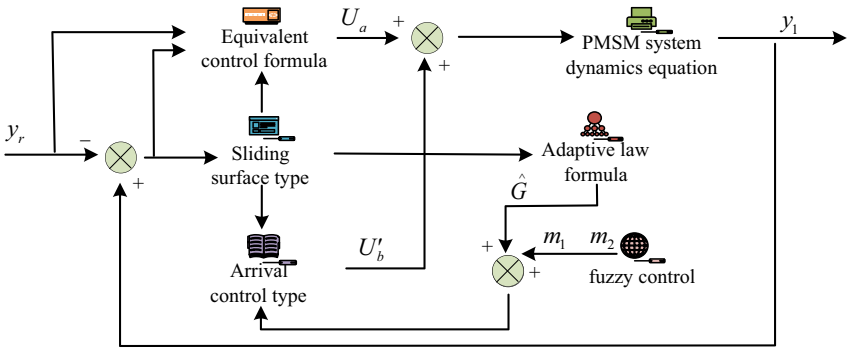

FIGURE 5. AFSMC system.

The formula of the center of gravity method is as Eq. (14).

$$\begin{cases} m_1 = \sum_{i=1}^{5} \alpha_i \beta_i \\ m_1 = \sum_{i=1}^{5} \mu_i \lambda_i \end{cases} \tag{14}$$

The adaptive law is designed according to Lyapunov's theorem, and the Lyapunov function is shown in Eq. (15).

$$V = \frac{1}{2\rho} s^2 + \frac{1}{2\mu_G} \tilde{G}^2 \tag{15}$$

In Eq. (15), $\rho = \beta\gamma_1 |e_2|^{\gamma_1 - 1}$, $\mu_G > 0$, $\tilde{G} = G - \hat{G}$, in which $\hat{G}$ denotes the upper bound estimate of parameter k_2, and $\hat{G}$ denotes the estimation error, which is calculated as shown in Eq. (16).

$$\tilde{G} = \begin{cases} \mu_G m_2 |s|^{\gamma_2 + 1}, & |s| \geq \Omega_0 \\ 0, & |s| < \Omega_0 \end{cases} \tag{16}$$

In Eq. (16), Ω_0 denotes the boundary layer thickness parameter of s; γ_2 denotes the boundary layer thickness parameter, which takes a positive value and is used to define the width of the boundary layer to avoid high-frequency jittering of the system on the slipmould surface; s adjusts the estimation of the upper bound of parameter k_2 when it is outside the boundary layer. s remains constant when it is inside, thus realizing the estimation of the upper bound of k_2. The AFSMC's flow is as Fig. 5.

In Fig. 5, first, the reference signal y_r is compared to the actual output y to generate an error signal. Secondly, this error signal is input into the sliding mode surface type module to generate control signals U_{k+1} and U_k. Then, U_{k+1} is processed through the equivalent control formula and enters the self-adaptive law control module together with U_k, which ultimately affects the dynamic equations of the PMSM system and achieves the precise control of the motor. Meanwhile, the fuzzy control module uses the G and $\tilde{G}$ signals to adjust the control parameters through the adaptive law formula to further optimise the system performance.

3.3. Stability and Controllability Analysis

Based on the proposed AFSMC strategy, a mathematical analysis was conducted to prove its stability, ensuring that the system remains stable under various operating conditions. Considering the nonlinearity and multivariable characteristics of the PMSM system, a Lyapunov function candidate was first constructed as shown in Eq. (17).

$$V(x) = \frac{1}{2} e^T P e + \frac{1}{2} \sum_{i=1}^{n} \lambda_i \tilde{G}_i^2 \tag{17}$$

In Eq. (17), e represents the error between the system state x and desired state x_d; P denotes a positive definite matrix; λ_i represents positive adjustment parameters. Based on the candidate function formula, the derivative of this function was further calculated to ensure that it is negative semi-definite or negative definite. According to the AFSMC control law and system dynamics, Eq. (18) can be obtained as shown,

$$e' = Ae + Bu + \Delta \tag{18}$$

In Eq. (18), A and B represent the system matrices, and Δ represents system uncertainties. By substituting the control input u, Eq. (19) can be derived as shown,

$$\begin{cases} u = -Ke - \text{sgn}(e) \\ e' = (A - BK)e - B\text{sgn}(e) + \Delta \end{cases} \tag{19}$$

In Eq. (19), K represents the feedback gain, and $\text{sgn}(e)$ represents the SM control term. Therefore, the derivative of $V(x)$ can be calculated as shown in Eq. (20).

$$\begin{aligned} V'(x) \ = \ & e^T P(A - BK)e - e^T PB\text{sgn}(e) \\ & + e^T P\Delta + \sum_{i=1}^{n} \lambda_i \tilde{G}_i' \tilde{G}_i \end{aligned} \tag{20}$$

To ensure the negative definiteness of $V'(x)$, the conditions shown in Eq. (21) need to be satisfied.

$$\begin{cases} e^T P(A - BK)e < 0 \\ e^T PB\text{sgn}(e) > 0 \\ e^T P\Delta < 0 \\ \sum_{i=1}^{n} \lambda_i \tilde{G}_i' \tilde{G}_i \leq 0 \end{cases} \tag{21}$$

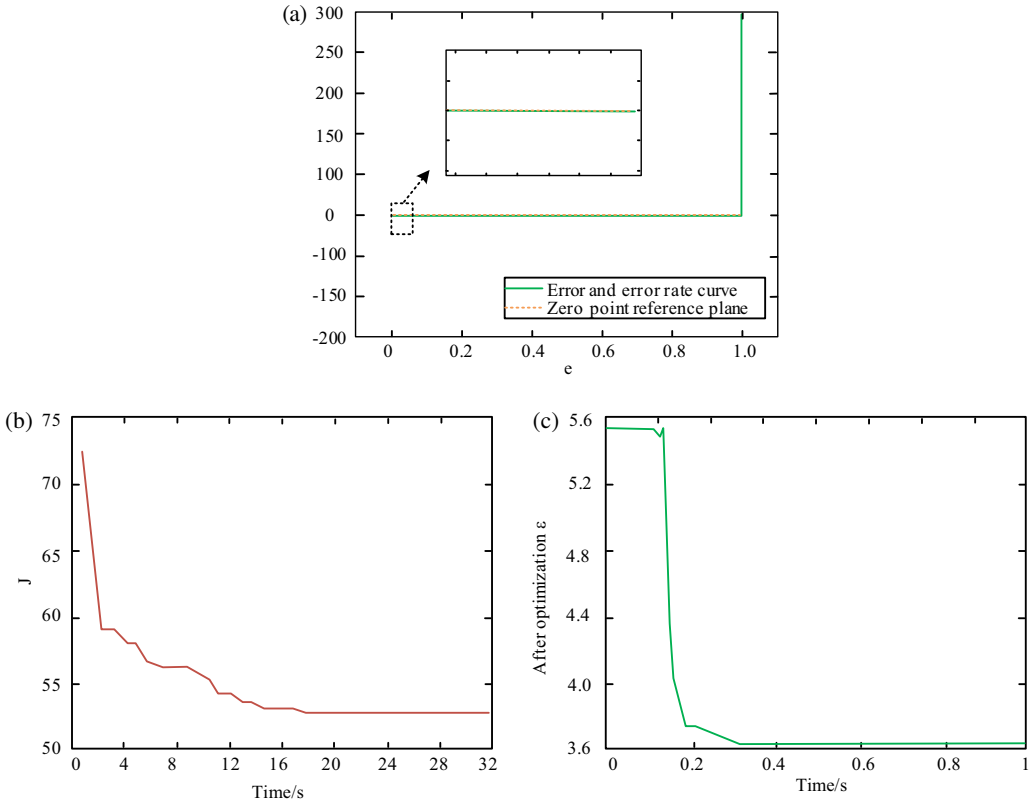

FIGURE 6. Verification results of adaptive fuzzy SM algorithm. (a) Error and error rate change curve. (b) Optimization process of objective function. (c) Parameter adaptive adjustment process.

Thus, by selecting appropriate positive definite matrix P and system matrix B, the above conditions can be guaranteed to hold, thereby proving the asymptotic stability of the system. On this basis, the controllability of the system was further analyzed. For the linear time-invariant PMSM system, the controllability matrix calculation formula is shown in Eq. (22).

$$C = \left[\begin{array}{cccc} D & AD & A^2D & A^3D \end{array} \right] \tag{22}$$

In Eq. (22), D represents the input matrix, and the specific calculation formula is shown in Eq. (23).

$$D = \left[\begin{array}{c} 0 \\ \frac{1}{L} \\ 0 \\ 0 \end{array} \right] \tag{23}$$

In Eq. (23), L represents the inductance. This matrix describes how the control input affects the system's state. The calculation formula for the system matrix A is shown in Eq. (24).

$$A = \left[\begin{array}{cccc} 0 & 1 & 0 & 0 \\ 0 & 0 & -\frac{1}{L} & 0 \\ 0 & 0 & 0 & 1 \\ 0 & 0 & -\frac{K_t}{J} & \frac{D}{J} \end{array} \right] \tag{24}$$

In Eq. (24), K_t represents the torque constant, and J represents the moment of inertia. By substituting A and D into Eq. (22), Eq. (25) can be obtained.

$$\begin{aligned} C &= \left[\begin{array}{cccc} D & AD & A^2D & A^3D \end{array} \right] \\ &= \left[\begin{array}{cccc} 0 & 0 & 0 & -\frac{1}{L} \\ \frac{1}{L} & 0 & -\frac{1}{L} & 0 \\ 0 & 0 & 0 & 1 \\ 0 & -\frac{K_t}{JL} & 0 & 0 \end{array} \right] \end{aligned} \tag{25}$$

The rank of C is calculated $rank(C) = 4$, which indicates that the system is controllable. At the same time, it also shows that the control strategy proposed in this study can effectively control the system under certain conditions.

4. TEST AND ANALYSIS OF AFSMC BASED ON PMSM

4.1. AFSMC Algorithm Testing

To verify the effectiveness of the fuzzy rules after the optimization of the FA control algorithm, the study builds a PMSM vector control system and compares the FA control algorithms before and after the optimization, and the results are as in Fig. 6.

From Fig. 6(a), it is indicated that as the control process proceeds, the error value steadily diminishes, and the rate of change of the error stabilizes, with the final curve approaching the zero point. In Fig. 6(b), it can be seen that the objective function value J decreases gradually with the increase of time until it reaches a stable state. The curve changes in Fig. 6(c), on the other hand, reflect the dynamic adjustment process of the algorithm's parameters of the controller over time in a real control system. Fig. 6(b) shows the change of the objective function value seeking optimisation in the running time of the algorithm,

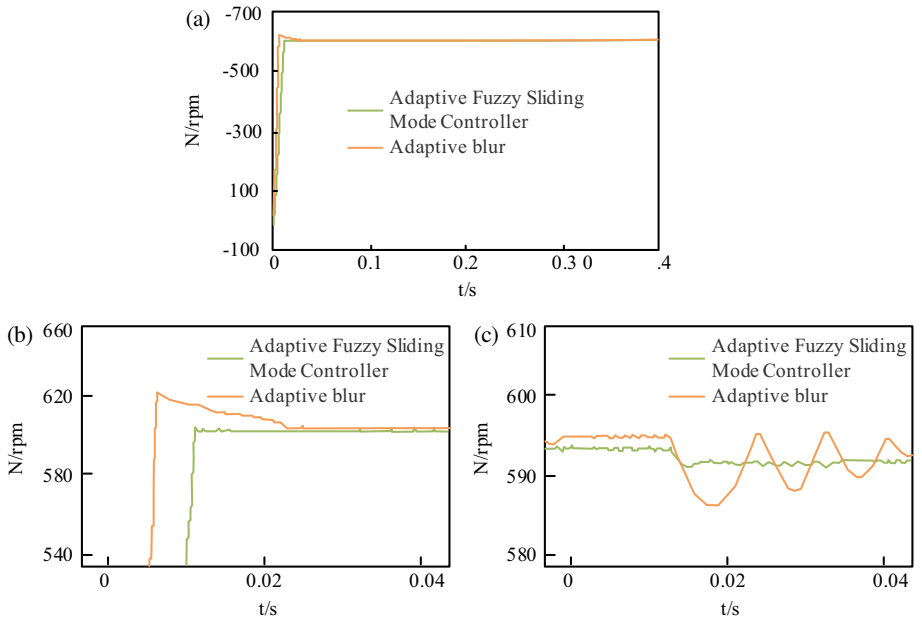

FIGURE 7. Comparison of adaptive fuzzy SM and adaptive fuzzy speed response. (a) Speed response curve. (b) Start up process curve. (c) Disturbance response curve.

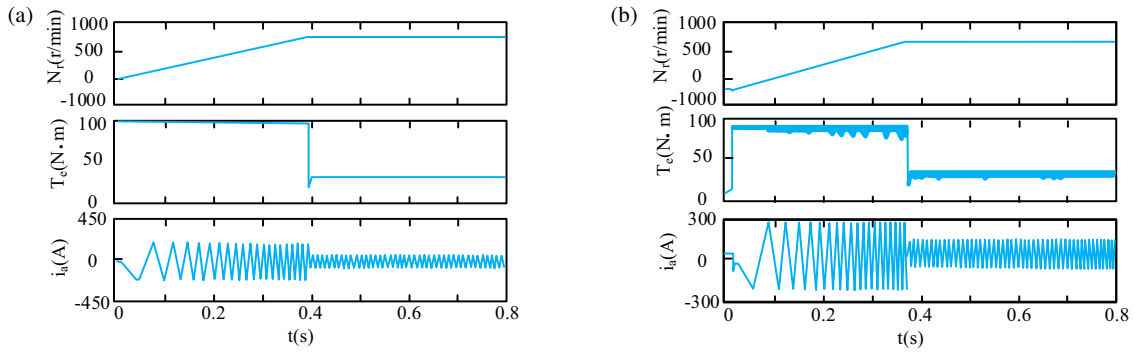

FIGURE 8. Comparison of algorithm performance curves under steady state. (a) Adaptive fuzzy synovial control steady state curve. (b) Adaptive fuzzy control steady-state curve.

i.e., the time consumed by the algorithm in the process of optimising the fuzzy rules, while Fig. 6(c) shows the time change in the actual control process. The trend of the three curves proves the stability of the system and the effectiveness of the control strategy. To test the performance of the improved AFSMC algorithm, the study conducts motor starting and loading experiments. The startup experiment examines the fast response and overshoot control of the AFSMC algorithm, and the loading experiment evaluates its anti-interference ability under load variation. In the experiment, the initial speed of the motor is 0, and it is set to 600 rpm after startup. 1.5 N-m load is added at 0.2 seconds, and the speed response is as Fig. 7.

In Fig. 7(a), the FA control reaches the stabilized speed in 0.023 s with an overshoot of 20 rpm, compared to the research-designed FA sliding film control, which quickly reaches the target speed in about 0.01 s, with almost no overshoot, and the speed is stabilized. In Fig. 7(b), even when the load is applied after 0.2 seconds, the motor speed decreases by only 2 rpm, which is much lower than the approximately 8 rpm fluctuation of the FA control. Therefore, the AFSMC not only maintains the fast response, but also solves the contradiction between fast response and overshooting, which obviously enhances the system's anti-interference ability and ensures that the rotational speed can still be stably maintained near the target value when the load changes.

4.2. Performance Validation of Adaptive Fuzzy SM and Adaptive Control

To confirm AFSMC's effectiveness, the study compares it with FA control in terms of both steady state performance and speed tracking performance, and the results are in Fig. 8.

A comparison of Fig. 8(a) and Fig. 8(b) shows that the AFSMC performance is more advantageous. When the motor is operated at 1500 rpm and a constant load of 305 Nm, the torque error of the FA adaptive control is only 5 Nm, and the peak torque pulsation is 35 Nm, while the torque error of the AFSMC is only 1.865 Nm. Compared with the FA adaptive control, the torque error and torque fluctuation of the AFSMC are reduced by 62.7% and 38%, respectively. Overall, the proposed

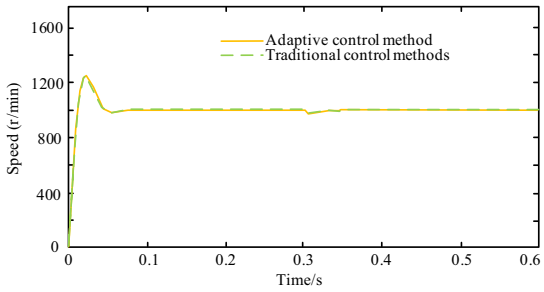

FIGURE 9. Parameter adaptive simulation results.

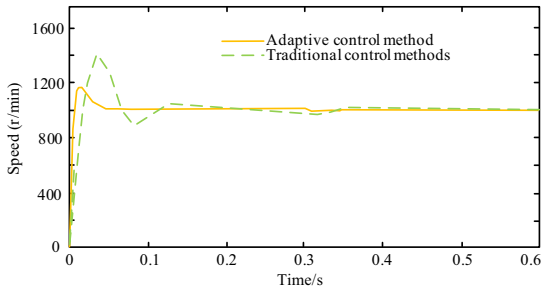

FIGURE 10. Comparison simulation results between adaptive and traditional controls.

TABLE 3. Validation of policy applicability in complex scenarios.

Control strategies	External interference		Parameter change	
	Amplitude of speed fluctuation (rpm)	Recovery time(s)	Amount of overshoot (%)	Adjustment time(s)
FA	±3.50	0.045	20.87	0.061
AFSMC	±1.20	0.018	5.33	0.022

AFSMC is superior in terms of response speed, load handling, electromagnetic torque, and current stability.

4.3. Simulation of Combined PMSM with AFSMC

To confirm the validity of the raised design method, the PMSM model is placed in the Simulink environment, and the motor parameters are changed to test whether the proposed method can increase the resilience of the PMSM during its operation.

In Fig. 9, the same parameters are used for both control methods during the period from 0 to 0.1 seconds. The system speed was set to 1200/minute when the motor was no-load, and the step response was tested. In the experiment, at 0.1 seconds, the resistance value of the motor stator winding increased by 30%, and the inductance value increased by 100%. At 0.3 seconds, a load torque of 10 Newton meters was applied to the motor while keeping the set speed and load torque constant. It is indicated that the two control methods have the same speed step response at the beginning of the system startup. In addition, at 0.1 seconds when the parameters were changed, the adaptive control method successfully recognized the parameters and adjusted the controller parameters accordingly. By 0.3 seconds, the motor speed under the conventional control method drops to 720 rpm and stabilizes after 0.03 seconds in case that the system is suddenly affected by the load torque. The motor speed under the adaptive control method, on the other hand, decreases to 970 rpm, but is stabilized after 0.01 seconds. It demonstrates that after changing the motor parameters, the adaptive control method can respond to the load changes faster than the traditional control method, and the former has better control effect and higher stability than the latter. This indicates that AFSMC is able to adjust quickly to maintain motor speed stability when parameters change, whereas conventional control methods take longer to stabilize. In the case of a sudden change in load torque, the AFSMC is able to recover to the set speed more quickly, whereas the recovery time for the conventional control method is significantly higher. Under the condition of keeping the parameters unchanged, the inertia of the system is set to 0.006 kg-m^2, and the traditional and adaptive methods are used to control the system. The test results are in Fig. 10.

By analyzing Fig. 10, it can be obtained that when the load inertia is kept constant, both the overshooting amount and regulation time are obviously more advantageous than the traditional control method. When the system inertia changes, the adaptive control method is also superior to the traditional control method, i.e., in the case of both of them, when the overshooting amount increases, the increase of the traditional control method is obviously greater than the adaptive control approach's. Moreover, the increase in regulation time of the adaptive control method is also less than the conventional control method. In addition to this, the amount of speed fluctuation is reduced when the inertia of the system increases, and the load increases suddenly, compared to the small inertia. In this case, the recovery time of the adaptive control method remains relatively stable, but the recovery time required by the conventional control method increases significantly, and the former can recover to the set speed faster than the latter. It can also be seen from Fig. 10 that the adaptive control method outperforms the conventional control method in terms of overshoot and regulation time when the load inertia remains constant. Even when the system inertia increases, and the load suddenly increases, the adaptive control method has less increase in overshooting amount, shorter regulation time, and better performance in terms of speed fluctuation. Finally, in order to further verify the applicability of the proposed AFSMC strategy, the study conducted experiments in complex scenarios with external disturbances and large parameter variations. The specific results are shown in Table 3.

As can be seen from Table 3, in the case of external disturbances, the fluctuation of the system speed is significantly

smaller than that of the traditional FA control method, and the recovery time is also shorter. In the case of large parameter changes, the AFSMC strategy can be quickly adjusted to keep the system running stably, while the traditional method has a large overshoot and longer regulation time. This proves the effectiveness and reliability of the strategy under complex working conditions.

5. CONCLUSION

To optimize the robustness of the FA control strategy in the PMSM, the study adopted the approach of combining the SM control technique with it. Through a series of experiments, it was verified that the AFSMC strategy significantly reduces the torque error to 1.86 Newton meters under the conditions of the motor running at 1500 rpm and subjected to a load of 30 Newton meters, which is 62.8% and 38% less than the conventional FA control strategy. This result not only proves the superiority of AFSMC in terms of steady-state performance, but also demonstrates its advantages in dynamic performance. In the robustness test, the performance of adaptive and conventional control methods was not much different in the early stage of system startup. However, when the motor parameters change, the former was able to recognize them and adjust the motor parameters in time. Unlike the adaptive control method, the motor speed of the system under the conventional control method decreases to 720 rpm at 0.3 seconds under the scenario affected by the load torque and returns to a steady state after 0.03 seconds. In complex scenarios, AFSMC reduces recovery time by 60% over traditional FA. Taken together, the application of the AFSMC strategy in the PMSM not only significantly improves the performance and stability of the system, but also demonstrates a stronger adaptive ability and control effect in the face of system parameter changes and external load fluctuations. However, there are some shortcomings in the study. For example, the PMSM model established in the study is derived under the idealized assumption of ignoring some non-critical factors. The real operating environment is extremely complex, and many factors are difficult to be accurately simulated, so the control strategy needs to be additionally adjusted and optimized in practical applications. Future research will consider the introduction of event-triggered mechanisms and stochastic modelling methods to further enhance the innovation and applicability of control strategies. These methods will help to reduce the update frequency of control signals and reduce the system communication burden, while improving the real-time performance and efficiency of the system. In addition, stochastic modelling methods will enable the control strategy to better adapt to complex and variable operating conditions.

ACKNOWLEDGEMENT

The research is supported by: National Natural Science Foundation of China (51777120); Carbon Peak and Carbon Neutral Special Programme for Science and Technology Support of Shanghai Science and Technology Innovation Action Plan 2021 (First Batch) (21DZ1207502).

REFERENCES

[1] Zhang, J., W. Zhan, and M. Ehsani, "Diagnosis and fault-tolerant control of permanent magnet synchronous motors with interturn short-circuit fault," *IEEE Transactions on Control Systems Technology*, Vol. 31, No. 4, 1909–1916, 2023.

[2] Li, Y., Q. Li, T. Fan, and X. Wen, "Heat dissipation design of end winding of permanent magnet synchronous motor for electric vehicle," *Energy Reports*, Vol. 9, 282–288, 2023.

[3] Yan, B., X. Li, X. Wang, Y. Yang, and D. Chen, "An improved 2-D subdomain method toward electromagnetic-performance analysis of line-start permanent magnet synchronous motor," *IEEE Transactions on Transportation Electrification*, Vol. 9, No. 3, 4339–4351, 2023.

[4] Xu, H., D. Yu, S. Sui, and C. L. P. Chen, "An event-triggered predefined time decentralized output feedback fuzzy adaptive control method for interconnected systems," *IEEE Transactions on Fuzzy Systems*, Vol. 31, No. 2, 631–644, 2022.

[5] Kumar, R., U. P. Singh, A. Bali, S. S. Chouhan, and A. K. Tiwari, "Adaptive control of unknown fuzzy disturbance-based uncertain nonlinear systems: Application to hypersonic flight dynamics," *The Journal of Analysis*, Vol. 32, No. 3, 1395–1414, 2024.

[6] Xu, B., Y.-X. Li, and C. K. Ahn, "Small-gain approach to fuzzy adaptive control for interconnected systems with unmodeled dynamics," *IEEE Transactions on Fuzzy Systems*, Vol. 30, No. 11, 4702–4716, 2022.

[7] Sui, S., C. L. P. Chen, and S. Tong, "Event-trigger-based finite-time fuzzy adaptive control for stochastic nonlinear system with unmodeled dynamics," *IEEE Transactions on Fuzzy Systems*, Vol. 29, No. 7, 1914–1926, 2020.

[8] Huang, H., C. Yang, and C. L. P. Chen, "Optimal robot-environment interaction under broad fuzzy neural adaptive control," *IEEE Transactions on Cybernetics*, Vol. 51, No. 7, 3824–3835, 2020.

[9] Yang, D., G. Zong, and S.-F. Su, "H∞ tracking control of uncertain markovian hybrid switching systems: A fuzzy switching dynamic adaptive control approach," *IEEE Transactions on Cybernetics*, Vol. 52, No. 5, 3111–3122, 2020.

[10] Zong, G., D. Yang, J. Lam, and X. Song, "Fault-tolerant control of switched LPV systems: A bumpless transfer approach," *IEEE/ASME Transactions on Mechatronics*, Vol. 27, No. 3, 1436–1446, 2022.

[11] Ren, H. R., H. Ma, H. Y. Li, and R. Q. Lu, "A disturbance observer based intelligent control for nonstrict-feedback nonlinear systems," *Science China Technological Sciences*, Vol. 66, No. 2, 456–467, 2023.

[12] Zheng, W., Y. Chen, X. Wang, R. Huang, M. Lin, and F. Guo, "Fractional order sliding mode control for permanent magnet synchronous motor speed servo system via an improved disturbance observer," *International Journal of Control, Automation and Systems*, Vol. 21, No. 4, 1143–1153, 2023.

[13] Rafaq, M. S., W. Midgley, and T. Steffen, "A review of the state of the art of torque ripple minimization techniques for permanent magnet synchronous motors," *IEEE Transactions on Industrial Informatics*, Vol. 20, No. 1, 1019–1031, 2023.

[14] Fang, S., Y. Wang, W. Wang, Y. Chen, and Y. Chen, "Design of permanent magnet synchronous motor servo system based on improved particle swarm optimization," *IEEE Transactions on Power Electronics*, Vol. 37, No. 5, 5833–5846, 2021.

[15] Yu, Y., Y. Pei, F. Chai, and M. Doppelbauer, "Performance comparison between permanent magnet synchronous motor and vernier motor for in-wheel direct drive," *IEEE Transactions on*

Industrial Electronics, Vol. 70, No. 8, 7761–7772, 2022.

[16] Wu, J., F. He, X. He, and J. Li, "Dynamic event-triggered fuzzy adaptive control for non-strict-feedback stochastic nonlinear systems with injection and deception attacks," *International Journal of Fuzzy Systems*, Vol. 25, No. 3, 1144–1155, 2023.

[17] Suganthi, S. and R. Karpagam, "Dynamic performance improvement of PMSM drive using fuzzy-based adaptive control strategy for EV applications," *Journal of Power Electronics*, Vol. 23, No. 3, 510–521, 2023.

[18] Dınakın, D. and P. Oluseyi, "Fuzzy-Optimized model reference adaptive control of interacting and noninteracting processes based on MIT and Lyapunov rules," *Turkish Journal of Engineering*, Vol. 5, No. 4, 141–153, 2021.

[19] Sun, X., F. Cai, Z. Yang, and X. Tian, "Finite position control of interior permanent magnet synchronous motors at low speed," *IEEE Transactions on Power Electronics*, Vol. 37, No. 7, 7729–7738, 2022.

[20] Shih, K.-J., M.-F. Hsieh, B.-J. Chen, and S.-F. Huang, "Machine learning for inter-turn short-circuit fault diagnosis in permanent magnet synchronous motors," *IEEE Transactions on Magnetics*, Vol. 58, No. 8, 1–7, 2022.

[21] Holanda, J., C. L. A. V. Campos, C. A. Franca, and E. Padrón-Hernández, "Effective surface anisotropy in polycrystalline ferromagnetic nanowires," *Journal of Alloys and Compounds*, Vol. 617, 639–641, 2014.

[22] Holanda, J., "Analyzing the magnetic interactions in nanostructures that are candidates for applications in spintronics," *Journal of Physics D: Applied Physics*, Vol. 54, No. 24, 245004, 2021.

[23] Silva, W. W. G., L. M. C. S. Hildever, M. C. G. Santos, F. Estrada, and J. Holanda, "Analyzing the magnetic influence on magneto-optical interactions," *Journal of Superconductivity and Novel Magnetism*, Vol. 36, No. 3, 951–955, 2023.